Power Electronics Powertrain Architectures for Hybrid and Solar Electric Airplanes with Distributed Propulsion

Damien Lawhorn, Vandana Rallabandi, and Dan M. Ionel, *FIEEE*
SPARK Lab, Department of Electrical and Computer Engineering
University of Kentucky, Lexington, KY, USA
damien.lawhorn@uky.edu, vandana.rallabandi@uky.edu, dan.ionel@uky.edu

Abstract

Distributed propulsion in aircraft has been shown to increase reliability and benefit aerodynamic performance. This paper discusses power electronic architectures and proposes control schemes suitable for distributed propulsion in hybrid and electric airplanes. Hybrid electric airplanes include permanent magnet synchronous generators driven by jet engines. The output of the generators is connected to the propulsion motors through back to back voltage source converters. Batteries, connected to the DC bus through buck-boost converters, are used to provide additional power to the propulsion motors during take off and climb. In the case of electric airplanes, the jet engine-permanent magnet generator system is replaced by solar photovoltaic (PV) panels. The output of the solar PV system is controlled such that it operates at its maximum power point, and power is provided to batteries and propulsion motors. Simulation results on both hybrid and solar electric systems are presented.

Index Terms – distributed propulsion, wide band gap semiconductor devices, solar photovolatic panels, permanent magnet synchronous machine.

I. Introduction

Distributed propulsion refers to airplanes with multiple thrust systems spaced along the wing and separated from the main engines. This aircraft design concept which is projected to improve take-off and landing performance, efficiency, reliability, noise and ride quality [1]. Distributed propulsion may be utilized in both hybrid and solar electric aircraft (Fig. 1). This paper discusses power electronic architectures suitable for hybrid and all-electric airplanes employing distributed propulsion. In the case of hybrid electric airplanes, the engine drives a generator whose output is rectified and feeds a DC bus. The DC bus powers the inverters which feed the propulsion motors. A battery, connected to the DC bus, discharges during times of take-off and landing, to supply the high power requirement of the propulsion motors, and may be charged at any time during the flight. Superconducting electric machines have been proposed for use in aircraft with distributed electric propulsion due to the high power density requirements [2]. Although the power electronic architectures and control strategies discussed in this paper pertain to permanent magnet machines, they can in principle be extended for use in conjunction with superconducting machines.

In the case of solar electric propulsion, the engine-generator is replaced by solar photovoltaic (PV) panels, and the surplus power is stored in a battery. A solar electric car, which also includes PV panels, batteries and propulsion motors has similar requirements. This paper also leverages and adapts a power electronics system architecture originally proposed for solar cars [3], to solar and hybrid electric airplanes.

II. Hybrid Electric Aircraft

Two electric airplanes are studied in this paper (Fig. 2 and Fig 3). The hybrid electric aircraft includes an engine which drives a vector-controlled permanent magnet generator whose output is rectified through a controlled AC-DC converter and feeds a DC bus. A battery is connected to the DC bus via a buck-boost converter. This powers the inverters which drive the propulsion motors. A higher DC voltage would potentially lead to reduced conductor weight for the aircraft. The control strategies employed for the power electronic converters are seen in Fig. 4. The generator side rectifier is fully controllable. The advantage of such an approach is that the currents of the generator can be controlled to be sinusoidal, and at the desired phase, leading to high efficiency and power factor. The active component of the generator current is controlled to maintain the DC bus voltage at its set value by the operation of the rectifier as follows,

$$I_q^* = (K_p + K_i/s)(V_{dc} * -V_{dc}), I_d^* = 0 \tag{1}$$

where, I_q is the q component of the generator current; K_p and K_i, the controller gains; V_{dc}^* and V_{dc}, the set and measured DC bus voltages respectively.

The d-axis component of the current is maintained at zero, for maximum torque per ampere. The position information required for the dq transformations is obtained from an encoder on the rotor, and sensorless control schemes can be used for

Table I
ELECTRIC AIRCRAFT, BASED ON [1],[4-9].

Aircraft	Turbogenerator [MW]	EMs [kW]	Batteries [kWh]	PV [kW]
NASA N3-X	30.600 (2)	4420.000 (14)	N/A	N/A
Airbus/Siemens/Rolls-Royce E-Fan X	2.000 (1)	2000.000 (4)	2000.000	N/A
Eviation Alice	N/A	260.000 (3)	900.000	N/A
Airbus E-Fan	N/A	30.000 (2)	29.000	N/A
Solar Impulse 2 (HB-SIB)	None	13.000 (4)	164.000	66.000
QinetiQ Zephyr 7	N/A	0.450 (2)	3.00	N/A
Autonomous Systems Laboratory AtlantikSolar	N/A	0.420 (1)	0.073	0.275

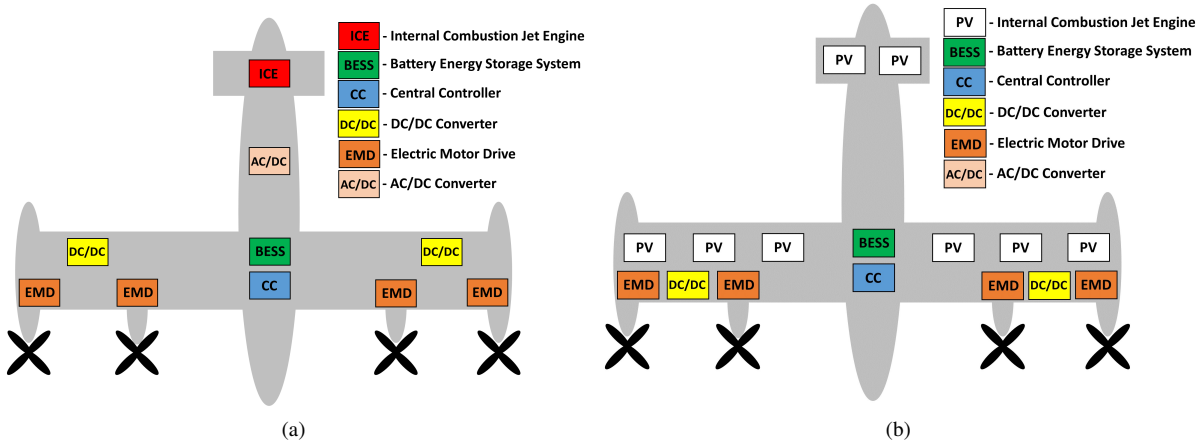

(a) (b)

Figure 1. Distributed powertrain for electric and hybrid airplanes. Inverters are placed at each motor. DC-DC converters are positioned along the wing. (a) HEA configuration includes the main system controller, jet engine, AC-DC converter, and battery which is located central on the aircraft. (b) SEA configuration includes solar panels distributed across the wings of the plane.

increased reliability. In case of the control of the motor side inverters, the active component of current is derived from the following,

$$I^*_{qm} = (K_p + K_i/s)(\omega * -\omega), \tag{2}$$

where, I_{qm} is the q component of the motor current; K_p and K_i, the controller gains; ω^* and ω, the set and actual motor speeds, respectively. The battery discharges during times of take-off and climb, to supply the high power requirement of the propulsion motors, and may be charged at any time during the flight. The battery side converter is bi-directional, and operates in the boost mode for discharging, and in the buck mode during charging. This enables the battery voltage to be smaller than the DC bus voltage. The battery current and duty cycle are derived from a power control loop, and the sign of the commanded power determines whether charging or discharging operation is desired. An alternative system configuration includes a multi-port isolated DC-DC converter which interconnects the rectifier output and battery energy storage (BES) with the propulsion motors and auxiliary loads (Fig. 5. The multi-port DC-DC (MPDCDC) includes a soft-switched DC-DC stage, operating at very high switching frequencies. A high frequency transformer is used to provide electrical isolation between the different ports. The high switching frequency serves to reduce the size of the transformer, and overall system filtering requirements. This converter topology may lead to increased reliability because of the galvanic isolation between the input and output stages. The MPDCDC is also versatile in the sense that additional ports may be added to accommodate loads at different DC bus voltages.

III. SOLAR ELECTRIC AIRCRAFT

The power required for aircraft propulsion in the solar electric case (Fig. 3), is provided by solar PV panels on the aircraft body. The PV panels are operated at the maximum power point by controlling the duty cycle of the boost converter that interconnects the panels to the DC bus (Fig.6). The input of the inverters driving the propulsion motors is tapped from the same nodes. A battery energy storage system is also connected to the DC bus via a bi-directional DC-DC converter. The duty cycle of the battery converter is controlled to maintain the bus voltage. The battery operates in the discharging mode when

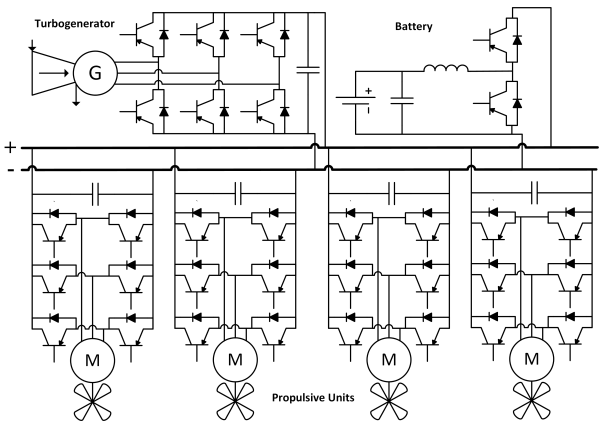

Figure 2. Schematic of power electronics architecture for a hybrid electric airplane. The electrical output of the turbo-generator is connected to the DC bus through a controlled rectifier. A battery is connected to the DC bus through a bi-directional boost-buck converter, and the inverters of the propulsion motor are fed through the DC bus.

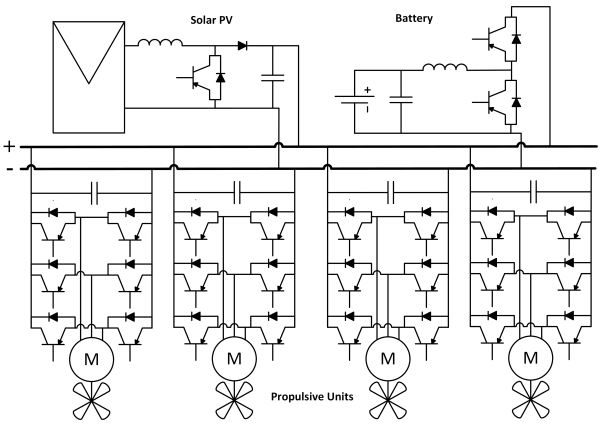

Figure 3. Power electronics architecture schematic for the solar electric airplane. The solar PV panel connects to the DC bus through a boost converter, which is controlled to operate it at the maximum power point. The battery is controlled to absorb excess power from the solar panels, and provide the power deficit during periods of high load and little solar availability.

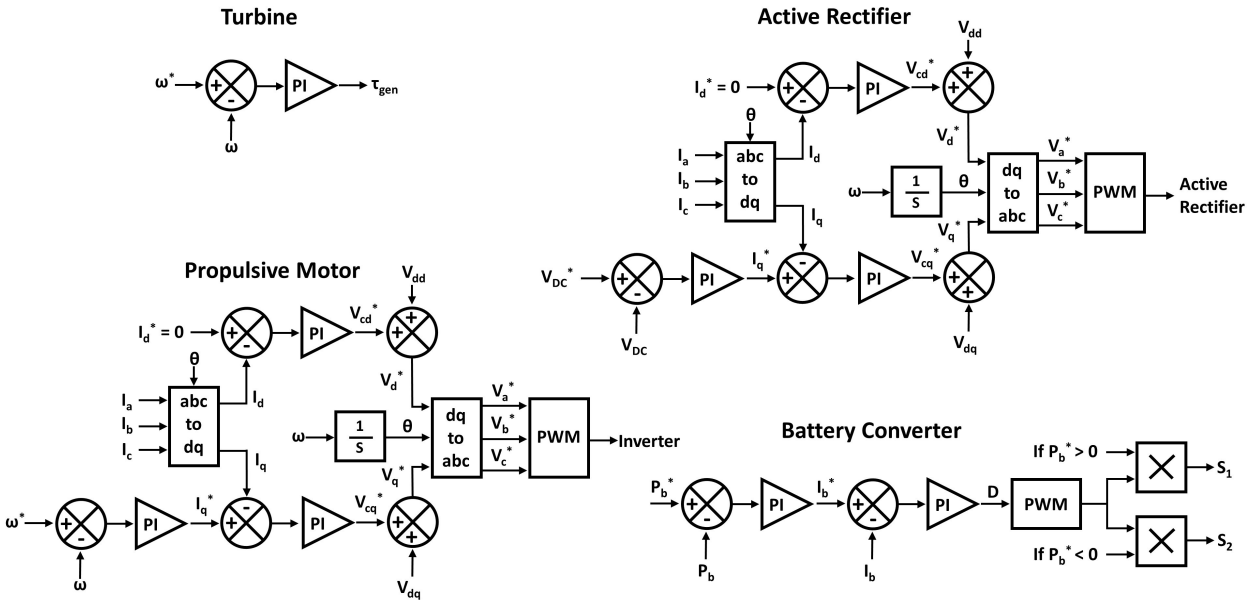

Figure 4. Control schemes for the turbine governer, generator side rectifier, battery and propulsion motor. The generator side converter maintains the DC bus voltage, and the battery charges when the flight is cruising. The battery can be controlled to discharge during take off and landing. The generator and motors and vector controlled, and position information for the transformations is derived from an encoder, or can be estimated sensorlessly for higher reliability.

the dc bus voltage falls below the set point, and in the charging mode when the DC bus voltage exceeds the reference value, as determined by the sign of I_b. Thus, the battery supplies the power deficit when the power from the solar panels is smaller than that required by the propulsion motors. During periods of high solar power and little load, the surplus power from the PV panels is stored in the battery. In case the battery's state of charge is at the maximum limit, and power from the solar panels exceeds the amount that can be absorbed by the propulsion motors, the duty cycle of the solar converter is modified to curtail the input power.

An alternative system configuration includes the MPDCDC converter previously discussed in the hybrid electric airplane section. In this configuration a multi-port isolated DC-DC converter interconnects the solar PV system and BES with the propulsion motors and auxiliary loads (Fig. 7). The MPDCDC of this system may serve the function of maximum power point tracking for the PV array.

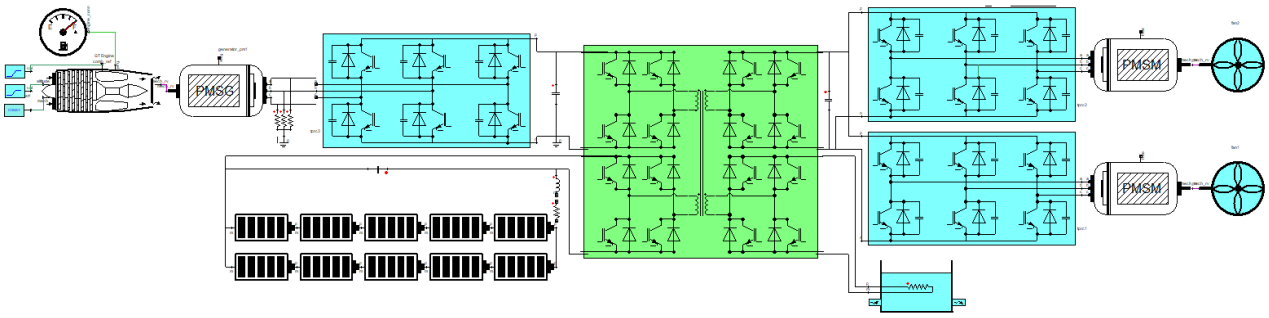

Figure 5. Hybrid Electric Aircraft (HEA) system architecture with jet turbogenerator, permanent magnet synchronous generator, propulsion motor and drive, battery, 4-port isolated high frequency DC/DC Converter, and auxiliary loads. In this implementation, the propulsion motors are fed from individual inverters connected to the same DC bus.

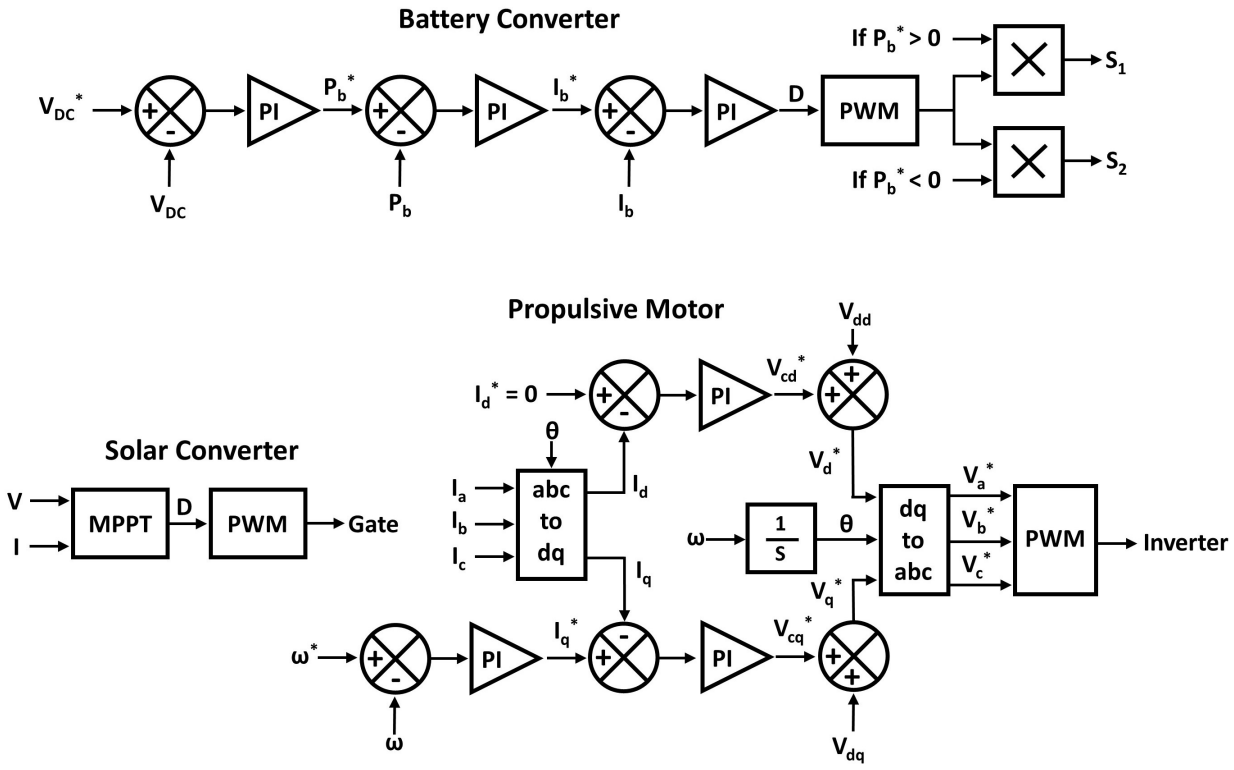

Figure 6. Control of the power electronic converters for the solar electric airplane. The solar side converter operates the PV system at the maximum power point. The battery converter regulates the DC bus voltage, and the traction inverters provide the required power to the motors.

IV. Simulation Results

Simulation of the system in Fig. 2 included driving the propulsion motors and generator over a given flight profile (Fig. 8a). The rating of the generator is 1MW, and the system includes 4-propulsion motors, each rated for 250kW. The DC bus voltage is considered to be 1.1 kV. The results for system power flow including power output from the motor, generator, and batteries are shown in Fig. 8. The flight profile shown represents the aircraft climbing to a stable low altitude, at which it cruises for 10 minutes. Upon leaving this stage, the aircraft ascends to a high altitude cruise, which it remains at for an additional 20 minutes. Next, the airplane begins the descent stage. Finally, another brief low altitude cruise is done before landing. The generator operates throughout the entire flight cycle. During the climb stages of the mission, the power demand from the propulsion motors is at its peak value. When a cruise altitude is reached, propulsion motor power demand is lowered. In such a situation, the battery is controlled to charge and non-operating propulsion motor propellers could be retracted to increase aerodynamic efficiency (Fig. 8(b)). During the descent stages, the required motor power is minimal. The battery is only required during periods of climb, and as the generator may provide power in other instances, its operation may be disabled after charging to

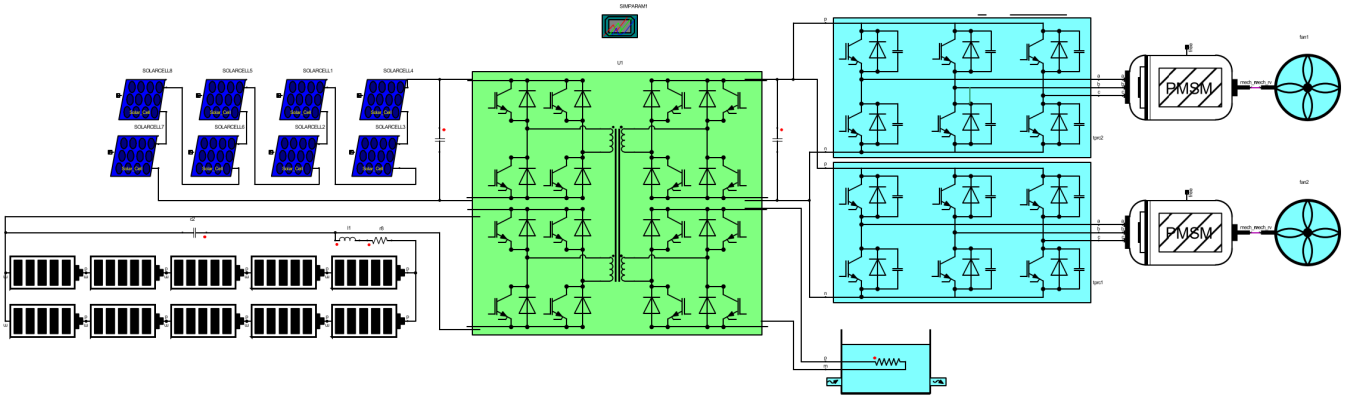

Figure 7. Solar Electric Aircraft (SEA) system architecture. System includes: permanent magnet synchronous machines (PMSM), motor drives, battery, 4pDC/DC Converter, PV array, and auxiliary loads. 4pDC/DC converter controls the power flow between the various components connected to the bus.

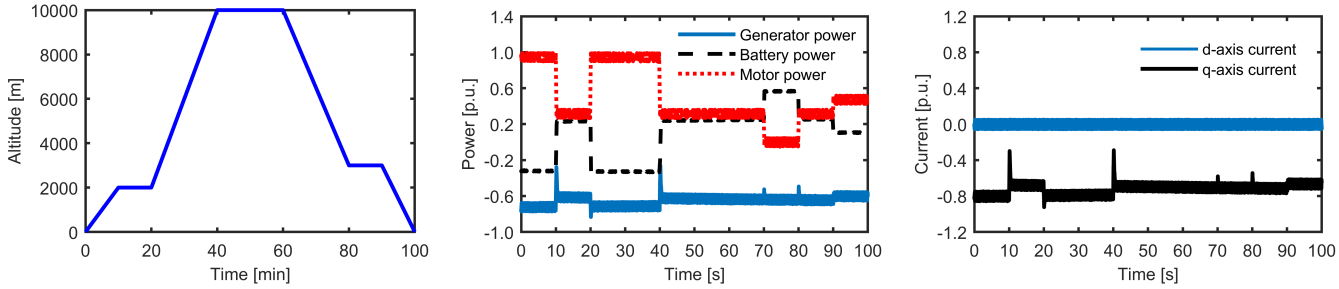

(a) (b) (c)

Figure 8. Simulations results of the HEA system. (a) Example flight profile of the mission, (b) Power flow of the generator, motor and battery under different operating conditions, with positive and negative signs corresponding to power absorption and delivery, respectively. (c) The d-axis current of the generator is always maintained at zero, while the q-axis current increases to supply the load of the propulsion motor, and battery.

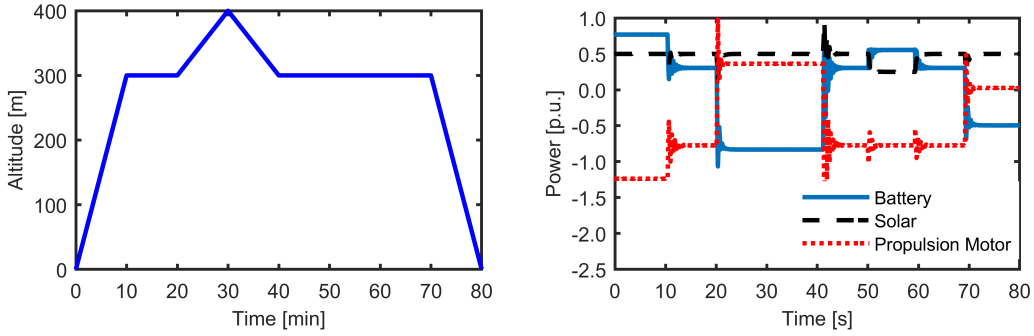

(a) (b)

Figure 9. Simulation results for the power flow of a solar electric airplane. (a) Example flight profile of the mission including a climb stage, regenerative soaring through thermal updraft, cruising, and landing. (b) Power flow between the components of the system. A 50% dip in irradiance occurs at t=50-60s.

full capacity to protect the system from overcharge damage. At t = 20min, the power demand from the propulsion motors increases, such an event may occur during take off and climb, and the battery discharges. At all operating instants, the DC bus voltage is maintained constant by the operation of the generator rectifier. Additionally, the generator currents are controllable as sinusoidal waveforms as can be inferred from Fig. 8 (c), which is achieved by the use of the controlled rectifier.

Simulation studies are also performed for the system of Fig. 7 for different conditions of solar irradiance and environmental situations. The flight profile and power flow is recorded (Fig. 9). The plane climbs to a low cruising altitude in search of thermal updrafts (Fig. 9a). During the climb the propulsion motor operates at its peak power. When reaching the cruising altitude, the required power drops to well below peak power. At t=20min the aircraft reaches a thermal updraft and the power to the propulsion motors is haulted. In this stage the aircraft gains altitude due to the thermal updraft. At t=30min the aircraft exits the updraft region and begins to descend to cruising altitude again. During this time period from t=20-30min the electric motors act as generators, sending power back to the battery. From t=50min-60min a solar irradiation dip of 50% occurs, at which point the battery output must supply the power demand difference. Beginning at t=70min, the aircraft glides to a landing using no power for the propulsion motors. The power flow of the flight cycle is shown in Fig. 9b. When the input solar energy is sufficient, it drives the propulsion motor as well as charges the battery and supplies auxiliary load. During periods of shading, the battery discharges to supply the required power to the motor as well as the auxiliary load. The BES also absorbs energy from the propulsion motor during regenerative soaring as suggested in [10]. The power flow in the MPDCDC converter is controlled by the phase shift between gating signals to the intermediate DC-AC stages. The phase shifts are controlled to operate the solar panels at the maximum power point, as well as achieve a power balance.

V. Conclusions

The paper discusses power electronics and control architectures for hybrid and solar electric vehicles. In the hybrid electric vehicle, the engine is driven by a synchronous generator whose output is connected to the DC bus through a controlled rectifier. A battery is also connected to the DC bus through a bi-directional DC-DC converter. The rectifier is controlled to maintain the DC bus voltage. The propulsion motors are driven from this bus, and the battery discharges when the power demand is high, such as during take off and climb periods. In case of the solar electric airplane, the DC bus is fed from solar panels, through a boost converter. Batteries are controlled to regulate the DC bus voltage. In addition, a multi-port DC-DC converter which provides galvanic isolation can be used for increased reliability. Simulation results are presented for two different flight profiles, including regenerative soaring in the case of the solar electric plane. Future work includes battery sizing, for both HEA and SEA systems. Additional work could be done on including fly-by-wire flight control systems as loads into the power system modeling.

Acknowledgment

The support of this research by the National Aeronautics and Space Administration, through the NASA Grant no. KY GF18020, University of Kentucky, the L. Stanley Pigman endowment, and ANSYS, Inc. is gratefully acknowledged.

References

[1] Nasa n3-x with turboelectric distributed propulsion. [Online]. Available: https://ntrs.nasa.gov/search.jsp?R=20150002081

[2] F. Berg, J. Palmer, P. Miller, M. Husband, and G. Dodds, Hts electrical system for a distributed propulsion aircraft, IEEE Transactions on Applied Superconductivity, vol. 25, no. 3, pp. 15, June 2015.

[3] V. Rallabandi, D. Lawhorn, J. He, and D. M. Ionel, Current weakening control of coreless afpm motor drives for solar race cars with a three-port bi-directional dc/dc converter, in 2017 IEEE 6th International Conference on Renewable Energy Research and Applications (ICRERA), Nov 2017, pp. 739744.

[4] M. Caujolle. Airbus, rolls-royce, and siemens team up for electric future partnership launches e-fan x hybrid-electric flight demonstrator. [Online]. Available: http://www.airbus.com/newsroom/press-releases/en/2017/11/airbus–rolls-royce–and-siemens-team-up-for-electric-future-par.html

[5] Alice commuter. [Online]. Available: https://www.eviation.co/alice/

[6] Airbus group: E-fan the new way to fly. [Online]. Available: company.airbus.com/service/mediacenter

[7] Technical challenges. [Online]. Available: http: aroundtheworld.solarimpulse.com/adventure

[8] B. C. Mecrow, J. W. Bennett, A. G. Jack, D. J. Atkinson, and A. J. Freeman, Drive topologies for solar-powered aircraft, IEEE Transactions on Industrial Electronics, vol. 57, no. 1, pp. 457464, Jan 2010.

[9] P. Oettershagen, A. Melzer, T. Mantel, K. Rudin, T. Stastny, B. Wawrzacz, T. Hinzmann, S. Leutenegger, K. Alexis, R. Siegwart, and et al., Design ofvsmall hand-launched solar-powered uavs: From concept study to a multi-day world endurance record flight, Journal of Field Robotics, vol. 34, no. 7, p. 13521377, 2017.

[10] J. P. Barnes, Flight without fuel regenerative soaring feasibility study, in SAE Technical Paper. SAE International, 08 2006. [Online]. Available: https://doi.org/10.4271/2006-01-2422